Proton and neutron transition densities in ^{6,7}Li from low energy neutron and proton scattering

L. F. Hansen
Lawrence Livermore National Laboratory, Livermore, California 94550

J. Rapaport, X. Wang, and F. A. Barrios
Ohio University, Athens, Ohio 45701

F. Petrovich, A. W. Carpenter, and M. J. Threapleton
Florida State University, Tallahassee, Florida 32306
(Received 30 November 1987)

New elastic and inelastic neutron scattering data for ^{6,7}Li taken at 24.0 MeV have been analyzed in conjunction with existing proton scattering data for these targets at 24.4 MeV. The new data allow us to infer that $\rho_n \approx \rho_p$ in ^{6}Li and ^{7}Li in contrast with the results $\rho_n \approx (N/Z)\rho_p$ deduced from earlier proton and electron work.

A study of the nuclides ^{6,7}Li has been carried out with low energy neutrons at $E_n = 8$, 10, and 24 MeV.[1] Specifically, we have measured elastic differential cross sections for the $J^\pi = 1^+$ and $\frac{3}{2}^-$ ground states of these two targets and inelastic differential cross sections for the predominantly $J=2$ transfer $1^+ \rightarrow 3^+$ ($E_x = 2.184$ MeV), and $\frac{3}{2}^- \rightarrow \frac{1}{2}^-$ ($E_x = 0.478$ MeV) and $\frac{7}{2}^-$ ($E_x = 4.63$ MeV) transitions in ^{6}Li and ^{7}Li, respectively. This paper discusses inelastic transitions observed at 24 MeV. The present work complements another recent study of ^{6,7}Li which simultaneously considered weak and electromagnetic decay, electron scattering, and low energy (p,p), (p,p'), and (p,n) scattering data from these targets.[2]

The charge exchange data considered in Ref. 2 served mainly to fix the isovector $J=0$ and $J=1$ nucleon scattering amplitudes, while the γ-decay, (e,e') and (p,p') data were used to extract information on the $J=2$ proton and neutron mass transition densities. The essential idea for the latter is that the inelastic scattering cross sections are given schematically by[3]

$$\sigma_\alpha = R_\alpha^m \mid t_{\alpha p}^m \rho_p^m + t_{\alpha n}^m \rho_n^m \mid^2 \quad (\alpha = e,p,n) ,$$

where $t_{\alpha p}^m$ and $t_{\alpha n}^m$ represent the strength of the coupling between the probe α and the target protons and neutrons whose behavior is summarized by the transition densities ρ_p^m and ρ_n^m. R_α^m is a factor representing probe-dependent kinematical and dynamical distortion effects. Incident electrons determine ρ_p^m since $t_{en}^m \approx 0$. On the other hand, at the energy of these measurements incident protons have $t_{pn}^m \approx 3t_{pp}^m$ and are most sensitive to ρ_n^m. In using electrons and protons to obtain simultaneous information on ρ_p^m and ρ_n^m one is subject to absolute uncertainties in R_p^m, $t_{pp'}^m$, and t_{pn}^m. For incident nucleons at the energies considered here, $t_{np}^m = t_{pn}^m \approx 3t_{nn}^m = 3t_{pp}^m$ and R_n^m differs from R_p^m only through isovector effects in the elastic scattering potential of order $(t_1/t_0)(N-Z)/A$; therefore, the use of hadronic probes (p,p') and (n,n') to determine ρ_p^m and ρ_n^m is not sensitive to absolute uncertainties in the knowledge of R^m and t^m for nucleon scattering. Comparative studies of low energy (p,p') and (n,n') data have previously been used to map out ratios of moments of ρ_n^m and ρ_p^m for low-lying quadrupole transitions in medium mass nuclei.[4] A more detailed discussion of this problem can be found in Ref. 5.

The measurements were performed at the Ohio University beam swinger time of flight facility.[6] A 7.0-MeV deuteron beam, pulsed and bunched at a 5-MHz repetition rate with subnanosecond pulse width and average current of 3 μA, was focused into a 3-cm-long gas cell filled to 1.5 atm pressure and sealed with a 5-μm tungsten entrance window. The 24-MeV monoenergetic neutrons were produced via the ^{3}H$(d,n)^4$He reaction. The Li targets were cylinders, 2.54 cm in diameter and height, encased in 0.025-cm-thick stainless steel (SS) cylinders. Background measurements were done using an identical empty SS cylinder. The ^{7}Li material was 99.93% enriched, while the ^{6}Li was 94.73% enriched. The samples were located at approximately 14 cm from the neutron production source.

Neutrons were detected in a sevenfold array of NE213 liquid scintillator detectors, each 10 cm thick by 18.8 cm in diameter. The flight path from the scattering samples to the neutron detector array was 12 m. Pulse shape discrimination was used to eliminate gamma-ray events in the neutron detectors. The energy resolution was about 750 keV full width at half maximum. Individual measurements were normalized to the counting rate of a stilbene monitor detector situated 0.8 m from the neutron production source at a fixed angle ($\theta = -45°$) relative to the 0° line. Absolute cross sections were obtained by rotating the beam swinger to 0° and measuring the incident flux in the sevenfold array per monitor count, with the scattering sample removed. Only relative efficiencies of the neutron detectors are needed with this procedure.[6]

Data were taken in the angular range of 15°–140°. Typical time-of-flight spectra are shown in Fig. 1. Because the energy of the scattered neutrons from Li changes with angle by several MeV, a dynamic bias threshold setting was used. Measured relative efficiencies were used to correct the data. Other corrections applied to the extracted yield were anisotropy in the neutron source, flux attenuation in the sample, finite angular geometry due to sample size, and multiple scattering within the sample. The estimated errors in the absolute values of the differential cross sections are about 5% at the forward angles, increasing to 10–20% at some backward angles. The g.s. and first excited state (0.478 MeV) in ^{7}Li were not totally resolved. A sum of two peaks separated by the excitation energy was used to obtain the respective yields for angles larger than 60°. The peak shape was obtained from the analysis of the g.s. transition in ^{6}Li which resulted in a Gaussian shape slightly modified with a summation of Hermite polynomials. Data for the inelastic transitions are presented in Fig. 2, where they are compared with proton inelastic cross sections[2] at 24.4 MeV and the present calculations. As may be seen from Fig. 2, the neutron and proton differential cross sections have not only similar shapes, but also similar magnitudes. The exceptions are the

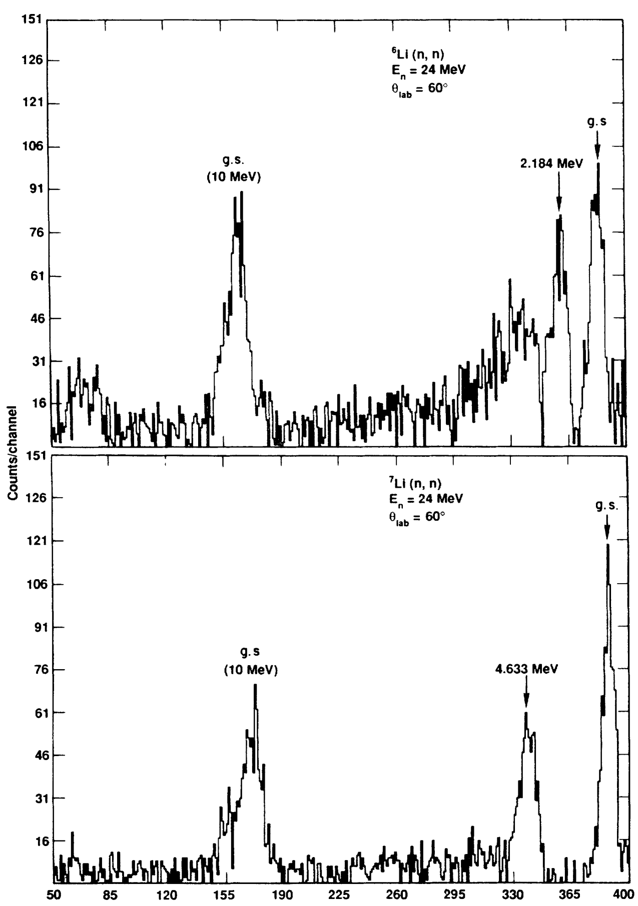

FIG. 1. Measured neutron time-of-flight spectra at 60° from the ^{6,7}Li(n,n) reactions at 24 MeV. From energy calibration, the peak position of the 0.478-MeV level in ^{7}Li is around channel 380. The peak around channel 170 in both spectra is the elastic peak from 10-MeV neutrons [produced in the ^{2}H$(d,n)^{3}$He reaction due to the presence of deuterium in the tritium target] scattered by the ^{6,7}Li targets.

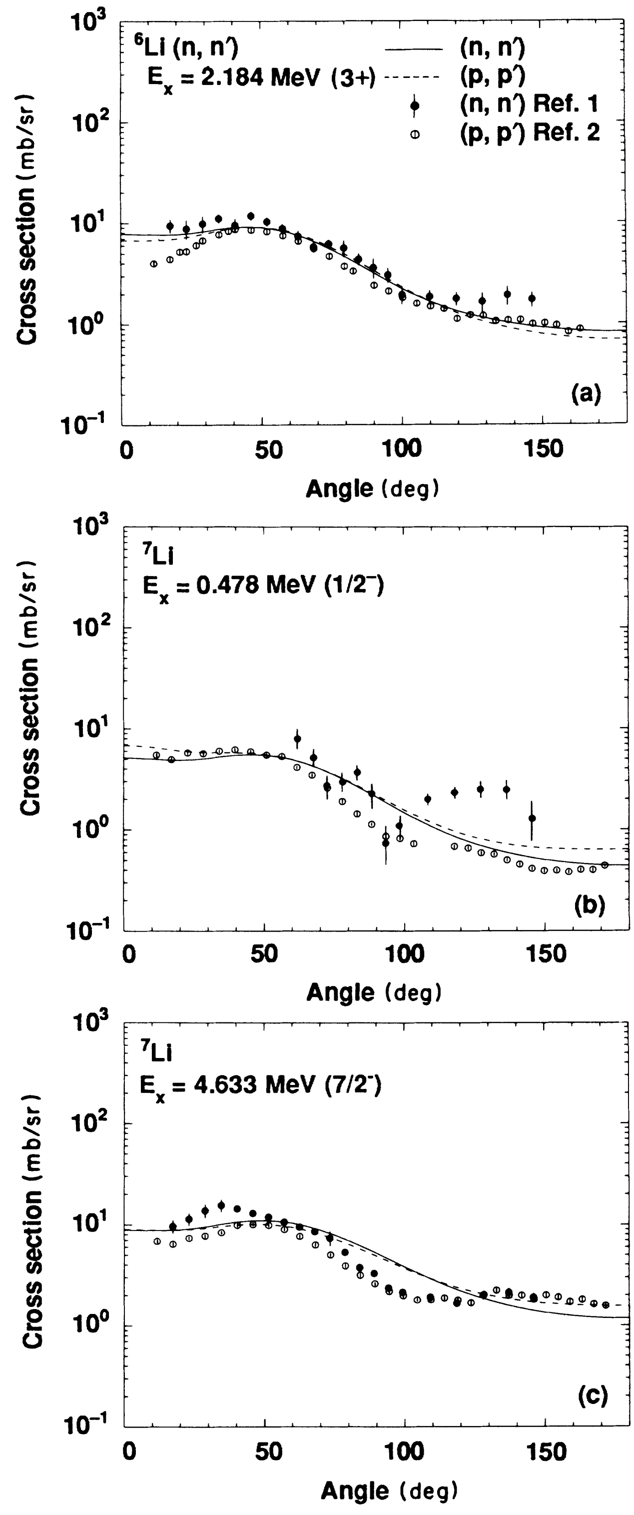

FIG. 2. Measured inelastic neutron and proton differential cross sections for the first (2.184-MeV) excited level of ^{6}Li and the first (0.478-MeV) and second (4.633-MeV) excited levels of ^{7}Li are compared with the theoretical results from the present work based on the new quadrupole enhancement factors given in Table I. The theoretical peak quadrupole cross section ratios are $\sigma_n/\sigma_p \approx 1.04$ and 1.09 for the first two ^{7}Li states, respectively. See text for details of the calculations.

TABLE I. Enhancement factors for quadrupole transitions in ^{6,7}Li deduced from electron, proton, and neutron scattering data.

Nucleus	Transition	Δ_p[a]	Δ_n[a]	ρ_n/ρ_p[a]	Δ_n[c]	ρ_n/ρ_p[c]
^{6}Li	$1^+ \rightarrow 3^+$	2.03	2.03	1.00	2.03	1.00
^{7}Li	$\frac{3}{2}^- \rightarrow \frac{1}{2}^-$	2.05	1.33	1.31	0.90	0.88
	$\frac{3}{2}^- \rightarrow \frac{7}{2}^-$	2.33[b]	1.51[b]	1.29	1.10	0.94

[a]Reference 2.
[b]Multiplied by 1.14 to correct error in Ref. 2.
[c]Present work.

^{7}Li$(n,n')^7$Li(0.478 MeV) data points which are higher than the reported (p,p) data for angles above 100°. However, the energy resolution was not good enough to separate these states.

The theoretical results of Ref. 2 were based on the preferred G matrix interaction of Bertsch *et al.*,[7] LS coupling shell model wave functions for the mass 6 and 7 targets,[8] and the phenomenological optical parameters of Bray *et al.*[9] determined for ^{6}Li. Isovector effects in the optical potential were neglected and the calculations were made with the code[10] DWBA70. Enhancement factors Δ_i were introduced to account for quadrupole renormalization effects not included in the shell model (SM) wave functions, i.e.,

$$\rho_i^m = \Delta_i \rho_i^m(\mathrm{SM}) \quad (i = p,n) .$$

The nucleus ^{6}Li has $N=Z$, so that $\rho_p^m(\mathrm{SM}) = \rho_n^m(\mathrm{SM})$ and $\Delta_p = \Delta_n$ from charge symmetry. The (e,e') and (p,p') data for this target were used to normalize the effective interaction. It was found that the $J=2$ differential cross sections had to be scaled by a factor $N=0.61$. For the two transitions of interest in ^{7}Li, $\rho_n^m(\mathrm{SM}) = 2\rho_p^m(\mathrm{SM})$. By adjusting Δ_p and Δ_n to reproduce the (e,e') and (p,p') data, it was concluded that $\rho_n^m \approx 1.3\rho_p^m$ for these cases. These results from Ref. 2 are summarized in Table I.

We have repeated the calculations of Ref. 2 and extended them to the present neutron scattering data. For ^{6}Li and ^{7}Li, respectively, we find the cross section ratios $\sigma_n/\sigma_p \approx 1$ and 0.72 without isovector effects included in the optical potential. With an estimate of the isovector potential based on $t_{pn} \approx 3t_{pp}$, which is consistent with the G matrix interaction of Ref. 7, we find $\sigma_n/\sigma_p \approx 0.83$ for ^{7}Li, compared to a value of about 1.15 ± 0.20 given by the data. Reconciliation of the theoretical and experimental ratios of the inelastic proton and neutron scattering cross sections for ^{7}Li requires a reduction in the values of Δ_n from Ref. 2 to increase σ_n/σ_p. These new values of Δ_n, which give ρ_n/ρ_p just less than unity, are also included in Table I. Since Δ_p is fixed from the electromagnetic data, the reduced values of Δ_n required to reproduce the experimental ^{7}Li σ_n/σ_p ratio produce absolute proton and neutron cross sections for ^{7}Li that are 0.64 and 0.83 times smaller than those obtained with the parameters of Ref. 2. Equivalently, we now produce the theoretical cross sections for mass 7, which are below the experimental values. The mass 6 cross sections are unaffected by the preceding considerations.

The theoretical inelastic proton and neutron scattering differential cross sections for the three transitions in ^{6,7}Li under discussion have been calculated using the new reduced Δ_n values with isovector effects included in the optical potential. Since the ground-state spin of each target is not zero, there are $J \neq 2$ unnatural parity contributions to each cross section. Details of the calculations of these unnatural parity transitions may be found in Ref. 2. Only the $J=1$ contribution to the proton cross section for the $\frac{3}{2}^- \rightarrow \frac{1}{2}^-$ transition in ^{7}Li has any particular importance, and this is limited to the forward angles. The total theoretical proton and neutron differential cross sections are compared with the 24.4-MeV (p,p') data of Ref. 2 and the present 24-MeV (n,n') data in Fig. 2. The theoretical results for ^{7}Li have been multiplied by 1.69 to bring them into agreement with the experimental data.

The results of new analyses[11,12] of the electron scattering data considered in Ref. 2 provide a resolution of the inconsistency of the normalization of the above theoretical results for ^{6}Li and ^{7}Li. These analyses point out deficiencies in the LS coupled shell model transition densities for the quadrupole transitions in ^{6,7}Li and provide improved phenomenological transition densities. These improved densities were used in calculations[11,12] for 200 MeV proton scattering from ^{6,7}Li and yielded consistent results. Specifically, the new transition densities produce ^{6}Li and ^{7}Li peak quadrupole cross sections at 200 MeV that are about 0.75 and 1.3 times those obtained with the LS coupling densities given in Ref. 2. These results indicate that with the new transition densities, a consistent description of the low energy (p,p') and (n,n') quadrupole transitions in ^{6,7}Li can be achieved by renormalizing the G matrix cross sections by $N \approx 0.80$, i.e., $N = 0.61/0.75$ and 0.61×1.3 for ^{6}Li and ^{7}Li, respectively.

In summary, new low energy neutron scattering data suggest that $\rho_n/\rho_p \approx 1$ for the three dominant quadrupole transitions in ^{6,7}Li in contradiction with earlier work based just on electromagnetic and low energy proton scattering data, which suggested that $\rho_n/\rho_p \approx 1.3$ for ^{7}Li. Inadequacies in the ^{6}Li model transition density used in the earlier work appear to be the source of the discrepancy. The constraint imposed by the neutron scattering data is critical in bringing these inadequacies into sharp focus.

This work was performed under the auspices of the U.S. Department of Energy by the Lawrence Livermore National Laboratory under Contract No. W-7405-ENG-48.

[1] L. F. Hansen, J. Rapaport, X. Wang, and F. A. Barrios, Bull. Am. Phys. Soc. **31**, 1237 (1986).

[2] F. Petrovich, R. H. Howell, C. H. Poppe, S. M. Austin, and G. M. Crawley, Nucl. Phys. **A383**, 355 (1982).

[3] F. Petrovich, J. A. Carr, and H. McManus, Ann. Rev. Nucl. Part. Sci. **36**, 29 (1986).

[4] A. M. Bernstein, V. R. Brown, and V. A. Madsen, Phys. Lett. **103B**, 255 (1981).

[5] J. A. Carr, F. Petrovich, and J. Kelly, *Neutron-Nucleus Collisions—A Probe of Nuclear Structure,* AIP Conf. Proc. No. 124, edited by J. Rapaport *et al.* (AIP, New York, 1985), p. 230.

[6] R. W. Finlay, C. E. Brient, D. E. Carter, A. Marcinkowski, S. Mellema, G. Randers-Pehrson, and J. Rapaport, Nucl. Instrum. Methods **198**, 197 (1982).

[7] G. Bertsch, J. Borysowicz, H. McManus, and W. G. Love, Nucl. Phys. **A284**, 399 (1977).

[8] S. Cohen and D. Kurath, Nucl. Phys. **73**, 1 (1965); **A101**, 1 (1967).

[9] K. H. Bray, M. Jain, K. S. Jayaraman, G. LoBianco, G. A. Moss, W. J. Van Oers, D. O. Wells, and F. Petrovich, Nucl. Phys. **A198**, 35 (1972).

[10] R. Schaeffer and J. Raynal, computer code DWBA70 (unpublished).

[11] C. W. Glover, C. C. Foster, P. Schwandt, J. R. Comfort, J. Rapaport, T. N. Taddeucci, D. Wong, G. J. Wagner, J. Seubert, F. Petrovich, A. W. Carpenter, and J. A. Carr (unpublished).

[12] A. W. Carpenter, F. Petrovich, R. J. Philpott, and J. A. Carr (submitted to Phys. Rev. C).